20-ps timing resolution with single-photon avalanche diodes

S. Cova, A. Lacaita, M. Ghioni, and G. Ripamonti

Politecnico di Milano, Dipartimento di Elettronica and Centro di Elettronica Quantistica e Strumentazione Elettronica CNR Piazza L. da Vinci 32 Milano, 20133 Italy

T. A. Louis

Heriot-Watt University Physics Department Riccarton, Edinburgh EH14 4AS, United Kingdom

(Received 7 November 1988; accepted for publication 14 February 1989)

Single photon avalanche diodes (SPADs) are avalanche photodiodes specifically designed for reverse bias operation above the breakdown voltage and used for detecting single optical photons. A new silicon epitaxial device structure was designed to give improved timing performance with respect to previous SPADs. Extensive tests were carried out in order to establish the timing resolution of the device in time correlated photon counting (TCPC). The timing resolution of the SPAD in terms of its full-width at half-maximum (FWHM) contribution to the overall instrumental response width is 20 ps with the detector cooled to -65 °C, and 28 ps at room temperature. This is the highest resolution so far reported for solid-state single-photon detectors. In vacuum tubes, comparable results are obtained only with special microchannel-plate photomultipliers (MCP-PMT). Results from time-resolved photoluminescence measurements in GaAs demonstrate the power of the TCPC technique when used with the new SPAD detector. With the excellent timing resolution of the SPAD and the well-known advantages of TCPC systems (high sensitivity, linearity, etc.), various applications are foreseen in areas so far dominated by streak cameras.

I. INTRODUCTION

The attractive features of the time-correlated photon counting (TCPC) technique[1] are nowadays widely known. TCPC is the technique of choice in most applications where fast, low-intensity optical signals must be accurately measured, particularly in fluorescence decay measurements. Since the advent of the synchronously pumped dye laser, ultrafast optical pulses have become readily available and hence the instrumental resolution of a TCPC system now depends mainly on the timing resolution of the detector. The full-width at half-maximum (FWHM) value of the instrumental response is commonly used to describe the timing resolution of a system. However, the accuracy with which decay time constants can be extracted from TCPC data by means of convolution analysis are typically 5–15 times better than the instrumental FWHM resolution value. This is due to the highly statistical nature of the TCPC data, which allows sophisticated convolution analysis techniques to be applied.[1] A similar, but much less dramatic improvement in time resolution can, at least in principle, also be obtained in ultrafast analog detection systems which use signal sampling (optical sampling oscilloscope), analog signal integration (phosphor screen in synchroscan streak camera) and/or postdetection averaging (all types of streak camera) for improving the statistical accuracy of the data. In these systems, subsequent simple deconvolution may improve the accuracy of the shortest measured time constant by a factor of 2 with respect to the FWHM resolution, but this is probably an upper practical limit. In this sense, a TCPC system with 50-ps FWHM resolution can be regarded as having an effective time resolution comparable to a synchroscan streak camera with 8-ps FWHM resolution.

The detector FWHM resolution is determined by the statistical distribution of the delay between the true arrival time of the photon at the detector, i.e., the SPAD junction or the PMT's photocathode, and the actual detection time as derived from the electrical output signal of the detector. If there are no further time-dispersive elements in the TCPC setup or provided their contribution to the instrumental FWHM resolution is accurately known, the FWHM resolution of the detector can be determined from the instrumental FWHM resolution. The ordinary fast photomultiplier tubes (PMTs), with electrostatically focused, discrete-dynode multiplier, have FWHM resolution values ranging from 600 to 120 ps.[2,3] A special type of PMT, with focusing by static crossed electric and magnetic fields, has produced instrumental FWHM resolution of 47 ps.[4] In recent years, reliable ultrafast PMTs with microchannel-plate (MCP) multipliers have become commercially available and detector FWHM resolution down to less than 30 ps was reported.[4,5] Solid-state devices, such as avalanche photodiodes (APDs) operated reverse biased above the breakdown voltage, can also be used for detecting single photons with high time resolution. In fact, some commercially available APD devices, originally designed for operation below the breakdown voltage in the amplifying mode, can also be used above the breakdown in the triggered avalanche mode. In particular, experimental investigations carried out on RCA C30921 S devices in a TCPC setup have demonstrated that these APDs give 400-ps FWHM resolution when cooled to -40 °C and 460-ps FWHM resolution at room temperature.[6] However, these values by no means represent the ultimate performance limit for such solid-state detectors. Much higher resolution is obtained with special avalanche devices, single photon avalanche diodes (SPADs), specifically de-

 0034-6748/89/061104-07$01.30

ned to work in the triggered avalanche mode.

Tests with early prototype SPAD devices[7–12] gave VHM resolution values down to 60 ps and demonstrated suitability of SPADs as TCPC detectors in applications ch as optical fiber characterization,[13,14] laser ranging, and orescence decay time analysis.[10–12] We have now designed d fabricated SPAD devices with a novel epitaxial struc-e[15,16] for improved timing performance. The design of the w devices is not only meant to improve the FWHM resolun value, but also to reduce the slow, wavelength-depennt tail that adversely affected the response shape of the ototype SPAD devices.[10–12] The remarkable results obned with the new device structure with respect to the rection of the tail are reported elsewhere.[15,16] In this article, report on the experiments that were carried out in order accurately determine the FWHM resolution of the new vices.

SINGLE-PHOTON AVALANCHE DIODES SPADS

SPADs are *p-n* junctions that can operate reverse biased ove the breakdown voltage. In this bias condition, a single rrier can trigger a self-sustaining avalanche current. In se of a photogenerated carrier, the leading edge of the avaiche pulse marks the arrival time of the detected photon. ie current will continue to flow until an external cirit[6,8–10] quenches the avalanche. The avalanche can also be ggered by thermally generated carriers in the depletion yer of the active junction. This effect causes the inherent rk count rate of the device. The dark count rate is further hanced by the presence of deep levels in the depletion layer ving rise to correlated afterpulses.[7,11,18] In order to avoid excessive dark count rate, the concentration of deep levels d other free carrier generation centers must be kept low by ıploying suitable fabrication processes.

We had previously implemented and tested prototype PAD devices using the geometry described by Haitz.[7–12] ieir response (Fig. 1) is characterized by a fast peak and a slow tail. The peak is caused by the carriers photogenerated within the depletion layer of the active junction. We observed and reported FWHM values down to 60 ps.[9–12] The experiments also showed that (i) the peak width is mainly related to the statistical fluctuations in the avalanche build-up time and (ii) the time resolution improves by increasing the maximum electric field in the active junction.[11] The tail is due to carriers photogenerated in the neutral region below the active junction, some of which reach the active junction considerably delayed, after diffusion.[17]

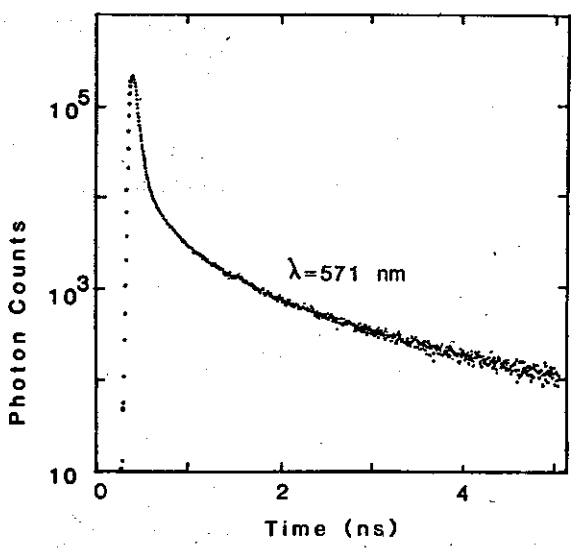

G. 1. Typical resolution curve of a prototype SPAD device, measured th picosecond optical pulses from a cavity-dumped, mode-locked dye la- at 571-nm wavelength.

We designed a new device structure,[15,16] with active junction implemented in a p epitaxial layer grown over a *n* substrate. The reverse biased substrate-epistrate *n-p* junction effectively reduces the diffusion tail. In order to attain very high time resolution in the peak, maximum values in excess of 400 kV/cm are required to the electric field in the active junction. However, a very high electric field can significantly increase the dark count rate, since the carrier emission probability from generation centers is strongly enhanced by field dependent effects, such as the Frenkel–Poole effect and the phonon-assisted tunneling effect.[19] Since the primary goal was to investigate the resolution obtainable with this kind of device, it was decided to tolerate moderately high dark count rates, at levels acceptable in measurements on short time ranges.[1] The breakdown electric field was thus increased up to 550 kV/cm. The breakdown voltage of the new devices (about 13 V) is quite lower than that of the prototype SPADs (about 28 V) and the dark count rate is markedly higher. At room temperature, the dark count rate of the new epitaxial devices already attains several kpps at 1-V excess bias over the breakdown voltage; as the voltage is raised, it rapidly increases exceeding 100 kpps at 6-V excess bias. Prototype SPADs ranged from 100 to 1 kpps with 1-V excess bias and the increase with the bias voltage was slower. In order to fully exploit the higher resolution of the new SPADs, it was necessary to employ an active quenching circuit;[6,8–10] with simple passive quenching circuits, the performance of the device is severely degraded at high dark count rates.[6] All measurements reported in the following were performed at 6-V excess bias, which was found to give best FWHM resolution. At higher bias values the dark count rate becomes so high, that even with the active quenching circuit the detector performance degrades, due to the rising probability of a photogenerated carrier triggering an avalanche within the short but finite time ($\sim$30 ns) required to reset the SPAD device from quenched (or gated) state to standby. Any such event will produce an avalanche under ill-defined, i.e., low bias conditions, hence broaden the response and reduce the FWHM resolution.

II. ANALYSIS OF METHODS FOR TESTING RESOLUTION AND PRELIMINARY MEASUREMENT

The FWHM resolution of the epitaxial SPAD devices is expected to be a few tens of picoseconds. On this time scale, other sources of time dispersion will make significant contributions to the measured overall instrumental FWHM resolution. In order to obtain the true detector resolution, all other contributions must be independently measured and

then quadratically subtracted. Errors of the order of a few percent in these terms may well be significant. Some sources of time jitter may not even be exactly constant, in which case it may be a problem to obtain an accurate estimate of their contribution by a separate measurement. Consequently, if the quadratic sum of these terms is larger than the detector contribution, the evaluation of the detector FWHM resolution will be quite inaccurate. Possible alternative experimental set-ups were, therefore, carefully evaluated and results compared in order to identify individual sources of additional timing jitter and quantify their contribution to the overall instrumental FWHM resolution.

A. Waveform measurements

A straightforward method is the one commonly employed to measure the instrumental FWHM resolution of a time-correlated single photon counting setup for measurements of fluorescence decays. The waveform of a picosecond pulsed laser is measured; that is, the histogram of the time intervals between the onset of the optical pulse and the detection of a photon is collected. In the standard TCPC setup, suitable for low repetition rate light sources up to about 50 kHz, a standard electrical start signal, synchronous with the laser pulse, triggers the start input of a time to pulse height converter (TPHC). The standard stop pulse is provided by the single-photon detector and associated timing and pulse shaping circuitry. A multichannel analyzer (MCA) digitizes the amplitude of the output voltage pulses from the TPHC and collects the data from a large number of events in form of a histogram. The resulting histogram is essentially a discretized representation of the cross correlation function between two statistical distributions, namely, (i) the distribution of the start signals from the synchronism circuit and (ii) the distribution of the stop signals from the single-photon detector and associated circuitry with respect to the true onset of the optical pulse. Therefore, the overall instrumental FWHM resolution, i.e. the FWHM of the peak in the histogram, is given by the quadratic sum of the following contributions:

(a) the FWHM time-jitter of the start pulse with respect to the onset of the optical pulse;

(b) the optical pulse width;

(c) the FWHM resolution of the single photon detector, that is, the FWHM jitter between the true arrival time of the photon at the detector and the leading edge of the diode avalanche current;

(d) the additional FWHM time dispersion introduced by the circuit associated with the single-photon detector. Here, there is an essential difference between PMTs and SPADs. In the case of PMTs, the amplitude of the detector pulse has a statistical distribution. Since the risetime of the pulse is finite, if a finite-threshold comparator were used for producing a standard pulse it would introduce an additional time dispersion. Therefore, a constant-fraction discriminator (CFD) is normally employed in order to avoid this unwanted effect. In the case of SPADs, however, the detector output pulse has standard amplitude and shape, hence a CFD is not required. The comparator in the active quenching circuit merely adds dispersion arising from the trivial noise and drift sources in the circuit;

(e) the FWHM dispersion arising from trivial noise and drift in the TPHC circuit.

Gain-switched laser diodes are currently used in our laboratory as optical pulse generators. The optical pulse width of the fastest available module,[20] emitting at 785 nm, was not exactly known. The manufacturer quoted the pulse width to be better than 38 ps on the basis of the standard waveform measurement made with an ultrafast, microwave mounted *p-i-n* photodiode and a Tektronix sampling oscilloscope with S-4 sampling head, giving 65 ps FWHM resolution. The jitter of the synchronized electrical signal was said to be better than 10 ps, typically 5 ps. For comparison, we also used a mode-locked and cavity-dumped dye laser system, previously employed in fluorescence decay measurements with SPAD detectors.[10] With Rhodamine 6G, optical pulses with less than 5 ps FWHM at 571 nm were obtained, as measured with an autocorrelator based on second harmonic generation. The electrical synchronization signal was obtained by splitting off part of the laser beam onto a fast *p-i-n* photodiode (HP 5082-4220). Since the amplitude of the dye laser pulse was not constant but statistically fluctuating by about 10%–15%, a CFD was used to derive a standard pulse from the photodiode signal and minimize the time jitter. The residual start pulse jitter [term (a) above] was still believed to be significant. It was, therefore, accurately measured in the following way: a second *p-i-n* photodiode and CFD was set up in exactly the same way and driven by the same optical intensity. By using the output of the second CFD as stop for the TPHC, histograms were collected with FWHM from 40 to 45 ps, depending on the experimental conditions (laser intensity, etc.). The contribution of the TPHC [term (e) above], in our case an ORTEC model 566, was checked by applying a standard electrical pulse to both the start and the stop input: FWHM values less than 10 ps (typically, 7 or 8 ps) were found for counting times up to about 10 min. By quadratic decomposition the contribution of a single branch, i.e. the start pulse jitter, was found to be approximately 30–35 ps FWHM. The contribution from the active quenching circuit [term (d) above] was also measured. The output of a fast electrical pulse generator was split up and fed into two branches. The first directly drove the start input of the TPHC. The second was used to emulate the true SPAD signal in the active quenching circuit, connected to the stop input of the TPHC. A Tektronix sampling oscilloscope with a S-4 sampling head was used to preliminarily observe the leading edge of the current pulses produced by the SPAD when operated under normal conditions, i.e., biased 6 V above the breakdown. The SPAD was then biased just below the breakdown voltage. The SPAD was kept connected to the active quenching circuit in order not to disturb the balance of impedances at the AQC comparator inputs and an artificial current pulse, adjusted such as to emulate the SPAD signal, was injected at the AQC input by using a suitable passive attenuation network. The histograms collected in this test had about 16-ps FWHM. After quadratically subtracting the TPHC contribution, the AQC jitter was thus estimated to be about 14 ps.

In summary, it was concluded that in the waveform easurements the total additional time dispersion was about -40-ps FWHM. With the laser diode, the main contribu-n came from the width of the optical pulse, whereas with e synchronously pumped, cavity-dumped dye laser it was ie to the synchronization jitter in the start channel.

Autocorrelation measurements

In order to better exploit the ultrashort pulses of the nchronously pumped dye laser, the contribution due to the nchronism jitter should be avoided. To this aim, the TCPC t-up was slightly modified. As outlined in Fig. 2, the *p-i-n* otodiode and CFD of the start branch were substituted by econd SPAD and associated AQC, identical to the first, d the split-off laser beam was suitably attenuated. The CSPC setup now had identical start and stop branches hich permitted measurement of the autocorrelation func-n of the time distribution of the pulses from the SPAD and sociated AQC. The overall instrumental FWHM resolu-n recorded in the histogram was given by the quadratical m of the following contributions:

(c) same as above;

(c') same as (c), but arising from the the start detector;

(d) same as above;

(d') same as (d), but arising from the active-quenching rcuit of the start branch;

(e) same as above;

(f) the width of the optical pulse autocorrelation func-n.

With the synchronously pumped dye laser, the autocor-lation width of the optical pulse [term (f) above] was out 5 ps. The total contribution from noise sources in the ectronic circuitry, that is, the quadratic sum of terms (d), (d') and (e), was directly measured. The procedure was similar to that previously used to measure the term (d) alone. The output of the fast electrical pulse generator was again split up and fed into two branches. This time, however, both pulses were adjusted such as to emulate SPAD signals, one pulse was injected into the AQC in the start branch, the other one was symmetrically injected into the AQC in the stop branch. The histograms collected in this test had less than 25-ps FWHM. In summary, it was concluded that in the autocorrelation measurements with the synchronously pumped dye laser the total additional contribution to the FWHM resolution did not exceed 25 ps. Therefore, this test was expected to give the most reliable estimate of the detector resolution.

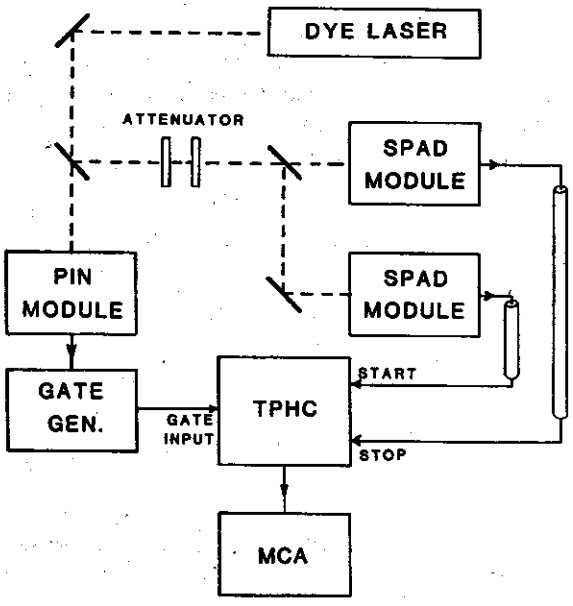

G. 2. Simplified block diagram of the experimental setup used in the autocorrelation measurements.

III. AUTOCORRELATION MEASUREMENTS WITH SYNCHRONOUSLY PUMPED DYE LASER

The experimental setup is shown in Fig. 2. The cavity dumper reduced the pulse repetition rate to 30 kHz. Neutral density filters were used to reduce the signal intensity to below the single photon level. The signal intensity was limited to produce a photon count rate 1.5 kpps (5% of 30 kHz) in order to prevent pulse pile-up effects. As mentioned in Sec. II, under standard test conditions of 6-V excess bias above breakdown, the dark count rate of the new epitaxial SPADs exceeds 100 kpps at room temperature. The high dark count rate caused some complication. Dark pulses in the start branch activate the TPHC which then, after time out or occurrence of a stop event, has to be internally reset. This causes the TPHC to be busy for a time interval of at least 10 μs (reset) following the start, and longer when a stop pulse occurs within the 50 ns conversion time range (conversion and reset). Hence, for a true photonic event in the start branch there is a high probability of the TPHC being busy due to a previous dark count event and, therefore, of being lost. This implies a long data collection time for obtaining a histogram with a sufficiently high number of counts in the autocorrelation peak. Apart from being unpractical, long data collection times are likely to produce data distorted by instrumental drift effects. Therefore, in order to avoid most of the useless starts, the TPHC fast gate facility was exploited. Another split off portion of the laser pulse train was directed to the fast *p-i-n* photodiode (HP 5082-4220) and CFD normally employed as start branch in the waveform measurements. The CFD output triggered a monostable circuit, that applied to the TPHC gate input a 100-ns square pulse, synchronized with the laser pulse. Start pulses were accepted only if they arrived within this 100-ns window. Coaxial delay lines were introduced into the start and stop branches. The TPHC start pulse was delayed with respect to the leading edge of the gating pulse by about 30 ns, the stop pulse was delayed another few nanoseconds with respect to the start pulse. These delays were necessary in order to have the start pulse well within the gate-on interval and for positioning the peak in the histogram well into the linear range of the 50-ns TPHC conversion window. In this gated arrangement, the circuitry of the TPHC start input was subject to less than 30 kHz pulse repetition rate. Of these, around 1.5 kcps were true photogenerated signals, the

rest were dark counts still. In the AQC a 3 μs deadtime was enforced in order to reduce the after-pulsing effect due to carrier trapping in deep levels.[7,11,18] In any gating arrangement, some photon pulses are inevitably lost, because of the deadtime associated with dark counts occurring during the 3-μs deadtime prior to the photonic event. Such losses can be greatly reduced by applying a pulsed bias voltage to the SPAD, that is, by directly gating the detector through the AQC (Ref. 21) instead of gating the TPHC, as was already shown in our previous tests on APDs.[6] With a gated detector, only the dark counts occurring in the short interval (a few tens of nanoseconds) between the opening of the gate and the occurrence of the laser pulse cause photon losses. In the present case, however, the simple gated TPHC arrangement was found to be sufficient, since a satisfactory histogram was collected in 10 min or less. Figure 3(a) shows the autocorrelation of the detector response, collected in 600 s, with 46 ps FWHM. Figure 3(b) shows the total experimental time dispersion due to noise in the electronic circuitry [the composition of terms terms (d), (d'), and (e), see Sec. III], with an autocorrelation FWHM of 24 ps. This was measured as described above, by using a mercury-wetted-relay pulse generator with low repetition rate. By quadratic decomposition, a 40-ps FWHM is obtained for the autocorrelation of the SPAD response. The FWHM resolution of the SPAD response at room temperature is, therefore, 28 ps.

IV. WAVEFORM MEASUREMENTS WITH LASER DIODES

Waveform measurements were first performed with the synchronously pumped dye laser. Histograms with FWHM values of 55 ps or more were obtained. Although the results did not provide new information, they were consistent with the analysis in Sec. II and the result of the autocorrelation tests. Extensive experiments were then carried out with fast laser diode pulsers. These results were compared with those obtained in the usual way, with an ultrafast *p-i-n* photodiodes connected to a sampling oscilloscope. From a practical standpoint, the measurements with the TCSPC were easier and faster, since a rough alignment of the laser diode with respect to the SPAD detector already gave a sufficiently high count rate. With a fast *p-i-n* photodiode, it is instead necessary to focus the available optical power onto the small *p-i-n* diode, which means careful, time-consuming alignment. From a performance standpoint, the experimental results confirmed that remarkably higher resolution and accuracy is obtained in the TCPC setup with the SPAD detector. In fact, the sampling oscilloscope measurements generally overestimated the pulse width. Furthermore, in various cases the latter did not reveal details of physical interest, such as small prepulses or after pulses, whereas these were clearly visible in the TCPC measurement with the SPAD detector. A typical example is shown in Fig. 4. The result of a measurement performed with the SPAD cooled to -65 °C is plotted; with the device at room temperature, the experimental curve was practically identical, but had 43-ps FWHM. The pulse-width of the 785-nm laser is evaluated to be 27 ps by quadratically subtracting the 28-ps FWHM of the SPAD (at room temperature, see Sec. III), the 16-ps contribution of the electronic circuitry and the 10 ps jitter of the electrical signal from the laser pulser (Sec. II) from the overall 43-ps FWHM. This is remarkably better than the 38-ps pulse-width estimated by the manufacturer on the basis of the sampling oscilloscope measurement. Furthermore, about 150 ps after the main pulse a small satellite pulse is clearly visible (probably due to a second cycle of the relaxation oscillation in the laser[22]), while it was obscured by electrical ringing at microwave frequency in the measurement with the fast *p-i-n* photodiode.

In the tests at low-temperature, the SPAD device was placed in a temperature-controlled chamber, the active quenching circuit and the 785-nm laser diode were kept out-

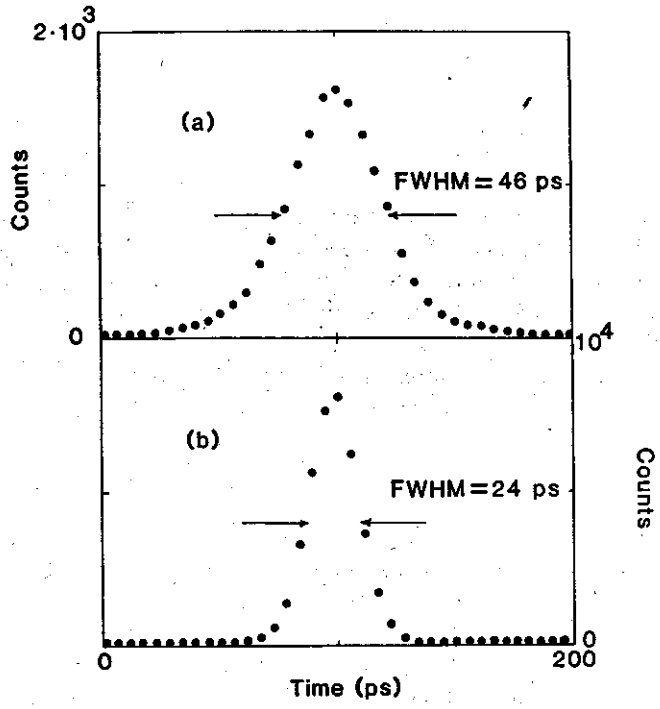

FIG. 3. Experimental histograms obtained with the set-up of Fig. 3: (a) autocorrelation of the overall detector response (SPAD and electronic circuitry); (b) time dispersion due to the electronic circuitry only.

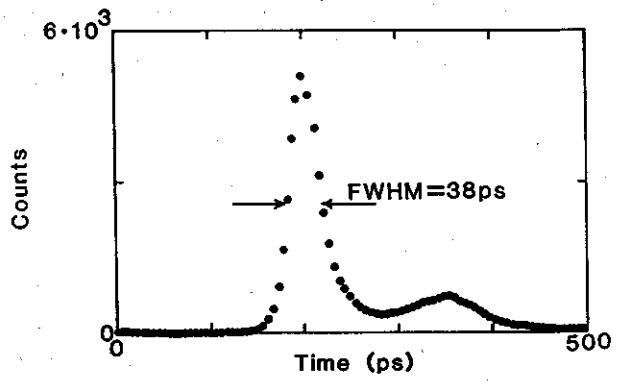

FIG. 4. Measurement of the waveform of a gain-switched laser diode emitting at 785 nm, performed with the epitaxial SPAD cooled at -65 °C and biased at 6V excess voltage above breakdown.

the chamber and coupled to the SPAD via coaxial cable optical fiber, respectively. The improved device perfor- ıce is ascribed to the higher efficiency of the impact-ioni- ɔn process in the semiconductor at lower temperature. ɹuadratically subtracting the 27-ps FWHM of the laser ɛ (see above), the 16-ps contribution of the electronic uits and the 10-ps synchronization jitter of the laser ɛr electrical trigger output (Sec. II) from the measured ıs overall FWHM, the FWHM resolution of the epitaxial ıD at − 65 °C is evaluated to be 20 ps or less. To the best ur knowledge, this is the highest resolution ever reported solid-state single-photon detectors. Comparable results ɛ been obtained only with special microchannel-plate tomultipliers (MCP).[5]

TESTS IN APPLICATIONS

The suitability of SPADs as single photon counting de- ors in measurements of fluorescence decays was demon- ted some time ago in experiments carried out with proto- ɛ SPAD devices.[10–12] The new epitaxial SPADs were also ed in the actual working conditions of TCPC setups for measurement of optical signals. A first test was per- ned on ultraviolet light signals, by measuring the pulse ɹeform of a coaxial flashlamp.[23,24] Figure 5 illustrates the ɔrovement in time resolution obtained with respect to measurements performed with a fast PMT in the same apparatus.[24] Further extensive tests were carried out in the near infrared on a recently developed novel TCPC system, the photoluminescence lifetime microscope spectrometer (PLuS). The PLuS is designed for high-resolution spatial mapping of time-resolved photoluminescence in compound semiconductors and is described in detail elsewhere.[25,26] A gain-switched AlGaAs laser diode was used to generate excitation pulses at 785-nm wavelength, less than 50-ps (FWHM) duration, 50-MHz repetition rate and approximately 2-mW peak power coupled into a single mode fiber pigtail. An epitaxial SPAD with a sensitive area of 5-μm diameter was used to detect gallium arsenide photoluminescence at 870 nm wavelength from samples held at room temperature. The temperature of the SPAD chip was monitored during the experiment and a Peltier cooler was used to actively stabilize the temperature of the SPAD to around 290 K. In cases where a lower dark count rate was required, the excess bias voltage above breakdown was lowered to 2 V, which limited the SPAD FWHM resolution to 50-ps FWHM. A commercial optical microscope was modified by insertion of a specially devised optical routing module in order to excite a sample area of 6 μm diam in the semiconductor sample and detect photons emitted from the central region with a lateral resolution of 3 μm. A typical result from a time-resolved photoluminescence measurement on a GaAs device is shown in Figure 6. The fit to the photoluminescence data was obtained by convolution of a three-exponential model function with the experimentally measured instrumental response and optimization of the fitting parameters by iterative, nonlinear least-squares analysis. In these time-resolved photoluminescence experiments with high-spatial resolution, the higher quantum efficiency of the SPAD with

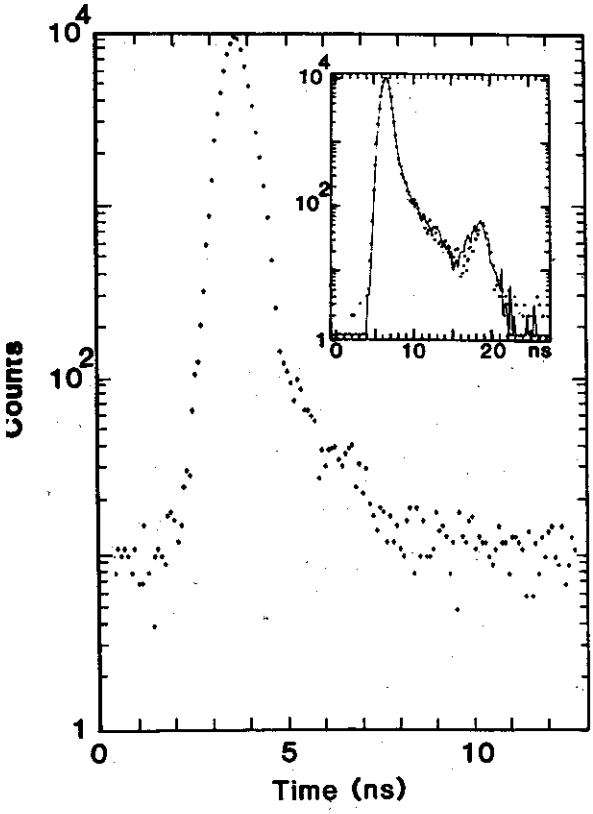

. 5. Optical pulseshape from a hydrogen-filled coaxial flashlamp,[23] mea- ɔd at 325 nm in a TCSPC setup with an epitaxial SPAD detector: the hlamp pulsewidth is 720 ps (FWHM). The inset shows, for comparison on a longer time scale, the result of a previous measurement obtained in same setup with a fast PMT (Philips XP2020Q)[24]: the measured ıewidth is 1370 ps (FWHM).

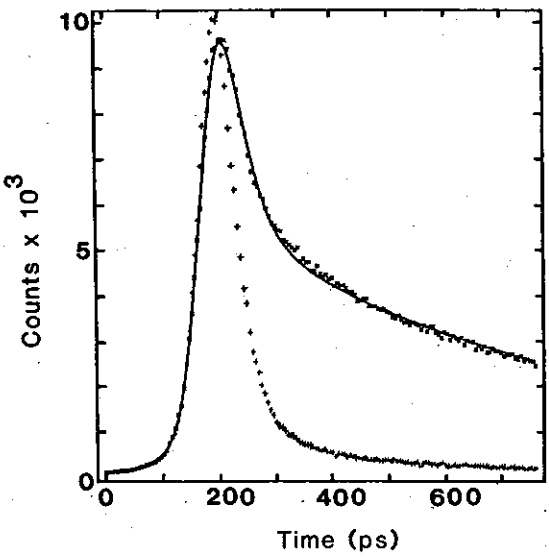

FIG. 6. Time-resolved photoluminescence response of a LPE grown homojunction GaAs solar cell as measured with the developmental PLuS system.[25,26] The figure shows the instrumental response at 785 nm (points marked +), the photolurninescence signal at 870 nm (points marked x) and the three-exponential fit obtained by convolution analysis (continuous line).

respect to vacuum tube detectors proved to be a valuable advantage. In fact, at the GaAs luminescence wavelength of 870 nm at room temperature, the internal quantum efficiency of silicon detectors is inherently higher than that of any photocathode material. Moreover, in this particular microscopic application, the small area of the SPAD detector was not a limitation at all. Work is in progress for the development of the photoluminescence lifetime microscope spectrometer (PLuS) and for producing other SPAD devices with still better characteristics. On the basis of the results so far obtained it can already be concluded that these new high-resolution solid-state detectors will open up new applications for the time-correlated photon counting technique in the picosecond regime, which was so far almost reserved to streak cameras.

ACKNOWLEDGMENT

The authors wish to thank D. Milesi for his work in the development of the active quenching circuit; M. Casiraghi for his assistance in the experimental tests; R. Cubeddu and R. Ramponi for the availability of the mode-locked laser system. This work was supported in part by Consiglio Nazionale Ricerche under programs "PF-MADESS Materiali e Dispositivi per l'Elettronica a Stato Solido" and "PS Fotorivelazione" and by Ministero Pubblica Istruzione.

[1]D. V. O'Connor and D. Phillips *Time-Correlated Single Photon Counting* (Academic, New York, 1983).
[2]V. J. Koester and R. M. Dowben, Rev. Sci. Instrum. **49**, 1186 (1978).
[3]S. Canonica, J. Forrer, and U. P. Wild, Rev. Sci. Instrum. **56**, 1754 (1985).
[4]D. Bebelaar, Rev. Sci. Instrum. **57**, 1116 (1986).
[5]H. Kume, K. Koyama, K. Nakatsugawa, S. Suzuki and D. Fatlowitz, Appl. Opt. **27**, 1 170 (1988). See also Technical Information No. ET-O3/Oct. 1987, Hamamatsu Photonics, K. K., Japan.
[6]A. Lacaita, S. Cova and M. Ghioni, Rev. Sci. Instrum. **59**, 1115, (1988).
[7]R. H. Haitz, J. Appl. Phys. **36**, 3123 (1965).
[8]P. Antognetti, S. Cova and A. Longoni, in *Proc. 2nd Ispra Nuclear Electronics Symposium*, Stresa, Italy, May 20–23, 1975 Euratom Publication EUR 5370e, pp. 453–456 (1975).
[9]S. Cova, A. Longoni, and A. Andreoni, Rev. Sci. Instrum. **52**, 408 (1981).
[10]S. Cova, A. Longoni, A. Andreoni, and R. Cubeddu, IEEE J.Quantum Electron. **QE-19**, 630 (1983).
[11]S. Cova, G. Ripamonti, and A. Lacaita, Nucl. Instrum. Methods A **253** 482 (1987).
[12]T. Louis, G. H. Schatz, P. Klein-Boelting, A. R. Holzwarth, G. Ripamonti and S. Cova, Rev. Sci. Instrum. **59**, 1148 (1988).
[13]G. Ripamonti and S. Cova, Electron. Lett. **22**, 818 (1985).
[14]C. G. Bethea, B. Levine, S. Cova, and G. Ripamonti, Opt. Lett. **13**, 23 (1988).
[15]M. Ghioni, S. Cova, A. Lacaita and G. Ripamonti, in *Proceedings of IEEE International Electron Device Meeting* (IEEE, New York, 1987) p. 452-455.
[16]M. Ghioni, S. Cova, A. Lacaita and G. Ripamonti, Electron. Lett. **24** 1476 (1988)
[17]G. Ripamonti and S. Cova, Solid State Electron. **28**, 925 (1985).
[18]S. Cova, G. Ripamonti, A. Lacaita, and G. Soncini, in *Proceedings of IEEE Int. Electron Device Meeting* (IEEE, New York, 1985).
[19]G. Vincent, A. Chantre, and D. Bois, J. Appl. Phys. **50**, 5484 (1979).
[20]PPL3OK Pulsed Diode Laser Modules, Opto-Electronics Inc., Oakville Ontario.
[21]S. Cova, A. Longoni and G. Ripamonti, IEEE Trans. Nucl. Sci. NS-2 599 (1982).
[22]K. Lau, Appl. Phys. Lett. **52**, 257 (1988).
[23]D. J. S. Birch and R. E. Imhof, Rev. Sci. Instrum. **52**, 1206 (1981).
[24]D. J. S. Birch, R. E. Imhof, and A. Dutch, Rev. Sci. Instrum. **55**, 125 (1984).
[25]T. A. Louis, Proc. Soc. Photo-Opt. Instrum. Eng. **1028**, paper No. 27 (in press).
[26]T. A. Louis, G. Ripamonti, and A. Lacaita (unpublished).